

Ar addition to CO₂ plasmas for controlling dissociation and vibrational excitation

A. Silva^{1,2,3}, A. S. Morillo-Candas², A. van de Steeg¹, O. Guaitella², V. Guerra³, G. van Rooij¹

¹ DIFFER (Dutch Institute for Fundamental Energy Research), part of the Netherlands Organization for Scientific Research, Eindhoven, the Netherlands

² LPP (Laboratory of Plasma Physics), École Polytechnique, Sorbonne Université, CNRS, Palaiseau, France

³ IPFN (Institute for Plasmas and Nuclear Fusion), Instituto Superior Técnico, Universidade de Lisboa, Portugal

Abstract: CO₂ dissociation is one of the problematic steps in the creation of solar fuels from this molecule. In this work the addition of Argon to CO₂ plasma is studied, namely how it affects dissociation and the vibrational excitation of CO₂. For this purpose, modelling and experimental investigation is carried out in order to understand the role of Argon addition, in these processes in continuous glow and pulsed microwave discharges.

Keywords: Ar-CO₂ plasma, plasma modelling, CO₂ dissociation, CO₂ vibrational excitation

1. Introduction

The transition from fossil fuels to more sustainable energy sources is an important subject nowadays. One of the possible solutions for the energy storage problem is the use of solar fuels: synthetic fuels produced from renewable energy sources. CO₂ can be used as a raw material but first the molecule has to be dissociated. This is a challenging task as that is a highly endothermic process. The use of non-thermal plasmas to activate the splitting of CO₂ has been recently under investigation, nonetheless the elemental kinetic processes occurring in this plasmas are not yet completely understood. However, this knowledge is key when it comes to finding ways to improve both conversion of CO₂ into CO and the energy efficiency of this process. One possible route to tackle the energy efficiency issue is to take advantage of the vibrational excitation of CO₂: through a V-V up-pumping mechanism [1], where successive collisions between vibrationally excited molecules further increase vibrational excitation, the dissociation limit can be reached with minimal heat loss in the process. In an effort to tune plasma parameters in a way that favours the vibrational excitation of CO₂, some studies were already done in CO₂ mixtures with rare gases [2-4].

In this work both continuous glow and pulsed microwave discharges are studied. The first provides an homogeneous and controlled medium, convenient for diagnostics and model validation, while the latter is seen as a more suitable set-up from an industrial application point of view. Both types of plasmas are investigated with diagnostics and simulations with the final goal of understanding what are the most relevant dissociation channels, what role CO₂ vibrations play, and how these are affected by Argon addition.

2. Experiments

Glow discharges are performed in a cylindrical reactor of 23cm length and 1cm radius. FTIR spectroscopy is used to measure *in-situ* conversion, gas temperature and vibrational temperatures of CO₂. The reduced electric field (E/N) is measured by probing the potential drop between two metal rods pointing radially inside the positive column

of the plasma. The results for different imposed pressures, currents, argon content and at a flow of 4 sccm are shown in Fig. 1-3.

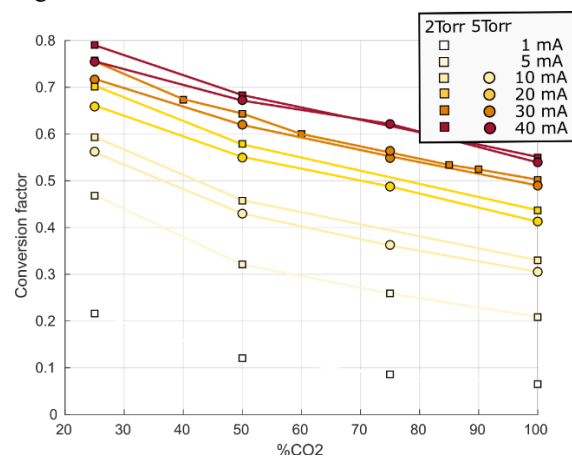


Fig. 1 CO₂ conversion as function of the % of Ar.

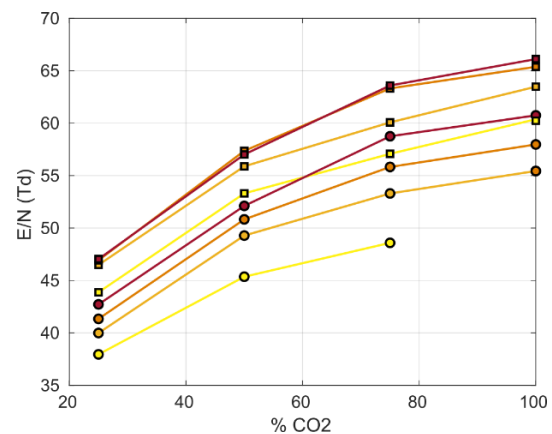


Fig. 2 E/N as a function of %Ar for glow discharge.

The measurements show that conversion improves with Argon addition, with its value increasing by about 20% for all the experimental conditions when adding 75% Ar to the mixture. Moreover, the reduced electric field drops significantly, about 20 Td from 0 to 75% Argon added. As for the gas and vibrational temperatures, the addition of

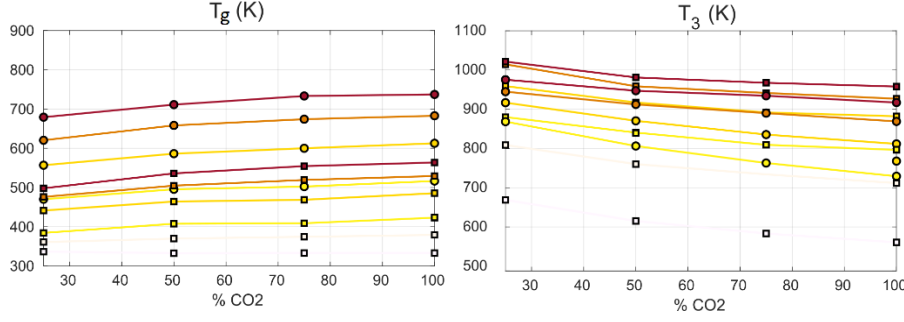


Fig. 3 Rotational and asymmetric stretch mode temperatures for glow discharge.

Argon does not seem to affect these quantities significantly, with changes relative to the pure CO₂ case always smaller than 20%. The qualitative behaviour is the same for all the working conditions: the gas temperature (T_g) remains about 100 K below the CO₂ bending and symmetric stretch mode temperature ($T_{1,2}$) and decreases as more Argon is added to the mixture; on the other hand, the temperature of the asymmetric stretch mode of vibration (T_3) increases with Argon content.

In the case of the pulsed MW plasma, the measurements are done at an excitation frequency of 2.45 GHz in a reactor with 1.3 cm of radius and at higher pressure, flow and input power (18.5 Torr, 4000 sccm tangentially injected and \sim 800 W peak power). The plasma is pulsed with a frequency of 30 Hz and has a ON time of 200 μ s. Vibrational temperatures of CO₂ and gas temperature are measured using Raman and Rayleigh spectroscopy, respectively. Scattered light and plasma emission are captured by a fast ICCD camera in order to get the time evolution of both temperatures and plasma dimensions in a μ s time scale. The forward and reflected power are both measured and the impedance is matched to minimize the power reflected in the first microseconds after ignition. Also, the plasma images are used to estimate the plasma volume in order to get the absorbed power density. The measured power densities and temperatures are plotted in Figs. 4 and 5, respectively.

It is observed that, while the power remains unchanged, the plasma volume increases as more Argon is added to the mixture. As for the gas and vibrational temperatures, while the former seems to be the same for all the working conditions, a higher vibrational non-equilibrium is achieved at higher fractions of the inert gas.

3. Modelling

For this work a kinetic scheme for the CO₂/Ar mixture is compiled from several published works [5-12]. This kinetic scheme is then implemented on LisOn KInetics [13]: a simulation tool that couples the solution of the Boltzmann equation for the electrons with the system of rate balance equations for the heavy species in the plasma. As schematically show in the code workflow in Fig. 6, the model requires as input an initial gas mixture, pressure, gas temperature, excitation frequency and electron density. For both discharges, all the quantities are measured except for

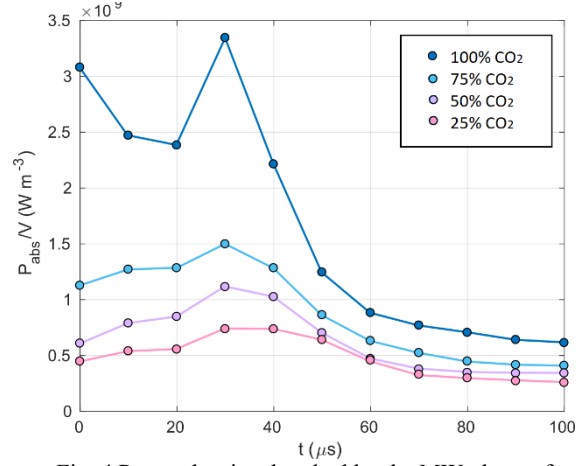


Fig. 4 Power density absorbed by the MW plasma for different mixture compositions.

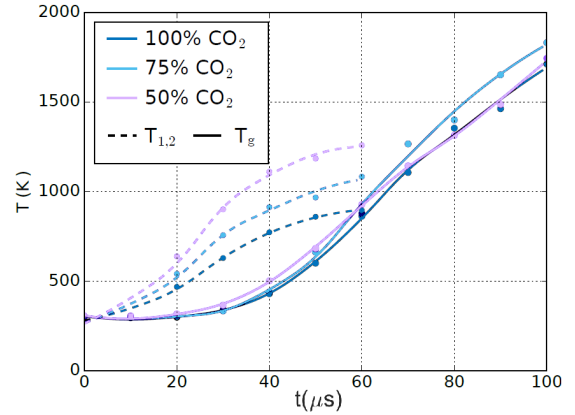


Fig. 5 Time evolution of gas and CO₂ bending and symmetric stretch mode temperature for the MW discharge.

electron density, which is estimated as:

$$n_e = \frac{I}{e v_d \pi R^2}, \quad (1)$$

in the case of the glow discharge, and as:

$$n_e = \frac{P_{abs}}{V} \frac{m_e (v_{n-e}^2 - \omega^2)}{v_{n-e} (E/N)^2 N^2} \times 2, \quad (2)$$

in the MW discharge case. In In these equations, v_d is the drift velocity of electrons, v_{n-e} the frequency of collisions between electrons and the neutral species, N is the gas

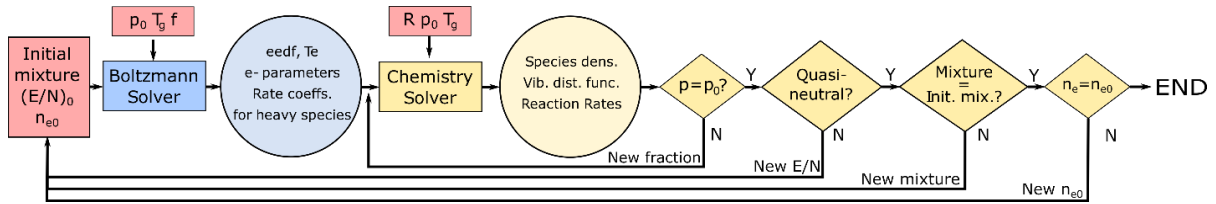


Fig. 6 Workflow of LoKI. After specifying pressure, gas temperature, field excitation frequency and an initial mixture, reduced field and electron density the Boltzmann solver retrieves the electron properties which, together with the chamber radius (R), are then passed to the chemistry solver. The rate balance equations for the heavy species are solved assuring that the pressure is kept constant, the plasma is quasi neutral, the mixture is consistent between the two simulation modules and the electron density calculated with Eq. (1) or (2) is consistent with the one given as input to the model.

density and E/N is the reduced electric field, which are outputs of the model. Moreover, I is the current passing through the plasma, R is the discharge radius, P_{abs} is the power absorbed by the plasma, V is plasma volume and ω is the field excitation frequency, which are experimentally measured quantities.

The kinetic scheme was validated with the measurements done in the glow discharge regime. A total of 130 experimental points are compared with the simulation results. The measured values correspond to working conditions in the range of 2 to 5 Torr, 1 to 40 mA, 4 to 10 sccm and 0 to 75% Argon content. The computed average difference between simulated and measured values of reduced electric field and conversion factors are about 10%. In Fig. 7 some results for fixed pressure and flow are represented.

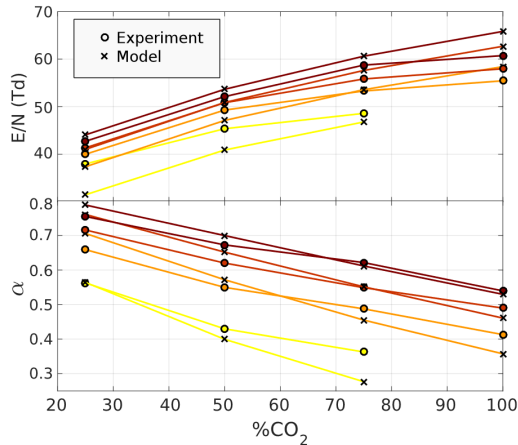


Fig. 7 Comparison between experimental data and simulation results at 2 Torr and 4 sccm.

The same model is used to characterize the MW discharge at different times along the pulse. This is done by running the simulation several times in steps of $10 \mu s$. For each time step, the inputs of the model are passed so as to be consistent with measured values - gas temperatures, plasma volume and absorbed power - as well as with the model's results in the previous time step - gas mixture. The EEDFs obtained for both glow and MW discharge are shown in Fig.8. The simulation results, for both the MW and glow discharge, point to the fact that the addition of Argon affects the plasma by changing the electron kinetics, although the effect is less apparent in the MW case. This is

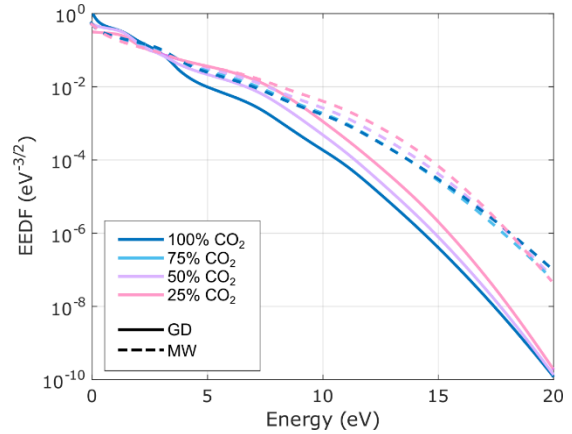


Fig. 8 Simulated EEDFs. The full lines correspond to the glow discharge regime at 2 Torr 10mA and 4 sccm and the dash lines to the MW case at 40μs.

coherent with the experimental results, which show that the only measured quantities changing significantly when changing the mixture are the electric field needed to sustain the discharge and the conversion of CO_2 into CO , which is mainly caused by electron impact. In fact, for the glow discharge case, it is found that the most important dissociative channels are dissociation by direct electron impact ($e + CO_2 \rightarrow e + CO + O$) and dissociative quenching of the first electronically excited state of CO in a collision with CO_2 ($CO(a) + CO_2 \rightarrow 2 CO + O$). According to the model's results these two processes are enhanced due to increasing electron impact rates of the first mechanism and of the electron impact excitation of CO , the main mechanism of $CO(a)$ production. These rates increase with Argon content due to the higher tail of the EEDF. At the thresholds of the electron impact processes just mentioned - about 7 eV - the EEDF computed for the glow discharge case is increased by almost one order of magnitude from the pure CO_2 to the 75% Argon case. Also, the electron temperature computed from these distributions, in the glow discharge case, grows from about 1 eV to 2 eV, while the estimated electron density does not change significantly.

In the case of the MW plasma, as the pulses are shorter than the time for significant electronic excitation of CO , all the dissociation is coming from direct electron impact. Moreover, due to the ionization degree, the EEDF is closer to a Maxwellian. The electron temperatures and densities

are significantly higher than in the glow discharge and the addition of Argon creates a less significant change in the EEDF. In Fig. 9 are plotted the simulated results for these quantities, as well as the conversion factors.

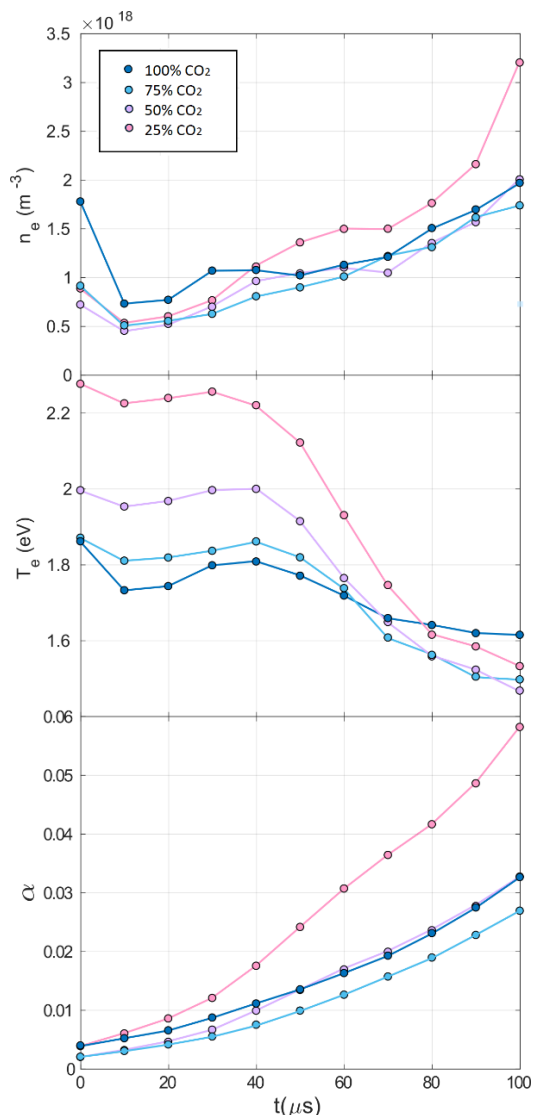


Fig. 9 Electron density and temperature and conversion factors obtained with the model for the MW discharge.

The most significant effect observed is on the electron temperature, which increases with Argon content due to its high threshold for electronic excitation, and in the self consistently computed reduced electric field, which increases from 80 to 140 Td in the first 100 μ s of the pulse in the pure CO₂ case, but only from 40 to 80 Td in the 25% CO₂ mixture.

The effect of Argon on vibrational excitation of CO₂ is still under investigation and the main conclusions so far are the ones taken from measurements: while no significant change in vibrational temperatures is observed in the glow discharge, in the MW case the excitation of the bending and symmetric stretch modes are enhanced with Argon addition. However, the change in electron kinetics predicted by the model is not expected to be beneficial for

electron impact excitation of the first vibrationally excited states of CO₂ in the case of the glow discharge, due to the significant depopulation of the bulk of the EEDF for higher Argon content. Yet, in the MW case, the calculated e-V rates corresponding to the excitation of the first three vibrational modes of CO₂ increase with Argon addition. That coupled with the poorer efficacy of V-T relaxation in CO₂-Ar collisions when compared with collisions between CO₂ pairs [14] is in agreement with the higher measured vibrational temperatures at higher percentages of Argon.

4. Conclusions

This work is focused in the use of diagnostics and models to study the CO₂ dissociation and vibrational excitation. The addition of Argon revealed to be beneficial for dissociation in the whole range of working conditions in which the glow discharge was operated. However, no significant changes in the vibrational excitation of CO₂ are observed. The preliminary results obtained for the pulsed MW plasma reveal a higher non-equilibrium of the bending and symmetric stretch mode of vibration for higher Argon content. The results of the modelling effort, validated by these experimental results, point to the conclusion that Argon addition to the CO₂ plasma significantly affects its the electron kinetics, increasing electron temperatures and decreasing the reduced electric field. As a consequence, the Argon addition increases the rates of electron impact dissociation of CO₂, which according to the model accounts for more than 75% of dissociation. Further understanding of the effect of Argon in the vibrational excitation of CO₂ from the modelling point of view requires a more extensive description of the vibrational kinetics that is still under development.

5. Acknowledgements

This work has been done within the LABEX PLAS@PAR project, and received the financial state aid managed by the ANR, as part of the programme "Investissements d'avenir" ANR-11-IDEX-0004-02. VG and LLA were partially supported by the Portuguese FCT under Projects UID/FIS/ 50010/2013, PTDC/FIS-PLA/1420/2014 (PREMiERE) and PTDC/FISPLA/ 1243/ 2014 (KIT-PLASMEBA)

6. References

- [1] P.A. Sá et al., Journal of Physics D: Applied Physics 37.2 (2003)
- [2] M. Moss et al., Plasma Sources Science and Tech. 26 03 (2017)
- [3] M. Ramakers et al., Plasma Processes and Polymers 12 8 (2015)
- [4] Y. Zeng et al., Journal of Physics D: Applied Physics 50 18 (2017)
- [5] A. Annusová et al., Plasma Sources Science and Tech., 27 4 (2018)
- [6] P. Ogloblina et al., XXXII ICPIG (2017)
- [7] J. Gregório et al., Plasma Sources Science and Tech. 21 1 (2012)
- [8] M. A. Ridenti et al., Physical Review E 97 1 (2018)
- [9] A. Yanguas-Gil et al., Journal of Physics D: Applied Physics 39 5 (2005)
- [10] IST database on LxCat. Accessed: 2018-03-03
- [11] P. Koelman et al., Plasma Processes and Polymers 14 4 (2017)
- [12] A. Cenian et al. Contribution to Plasma Physics 34 1 (1994)
- [13] A. Tejero et al., Plasma Sources Science and Tech. Accepted for publication (2018)
- [14] M. Huetz-Aubert and F. Lepoutre, Physica 78 (1974)